Polymer Chemistry

PAPER

Synthesis of Star-Shaped Polyzwitterions with Adjustable UCST and Fast Responsiveness by a Facile RAFT Polymerization

Received 00th January 20xx,
Accepted 00th January 20xx

DOI: 10.1039/x0xx00000x

Zhi Li, [a] Hao Li, [a] Zhonghe Sun, [a] Botao Hao, [a] Tung-Chun Lee, [b] Anchao Feng, [*a,c] Liqun Zhang [a,c] and San H. Thang [d]

Dual thermo- and pH-responsive star polymers with tunable upper critical solution temperatures (UCST) were synthesized by an "arm-first" RAFT polymerization approach. Crosslinking took place in a single step involving polymerization of 3-dimethyl(methacryloyloxyethyl) ammonium propane sulfonate (DMAPS) mediated by a macroRAFT agent containing carboxylic end-group and in the presence of crosslinker *N*,*N*-methylenebis(acrylamide) (MBA). Varied-temperature turbidity analysis, dynamic light scattering (DLS) and rheology analysis revealed that the star-shaped PDMAPS had a smaller hydrodynamic volume while retaining fast response properties, compared with linearly-shaped PDMAPS. Meanwhile, zeta-potential was used to determine that the range of UCST regulated by pH was greatly expanded and proportional to the number of end-groups that could be generally manipulated through RAFT polymerization. By changing the pH values from 3 to 10, the adjustable UCST range of the star polymer solution can reach over 36 °C. These results demonstrate that the topological structure and end-group effect are able to manipulate the phase transition behavior of polyzwitterions. These materials offer great potential as additives or drug delivery vehicles in biomedical applications.

Introduction

Zwitterionic polymers exhibiting stimuli-responsiveness are of great interest in biological applications.[1-7] Typically, linearly-shaped poly (3-((2-(methacryloyloxy) ethyl) dimethylammonio) propane-1-sulfonate) (PDMAPS) exhibits sharp and continuous phase change in aqueous solutions upon heating or cooling to an upper critical solution temperature (UCST).[8,9] The phase transition behavior of the solution is consistent with the aggregation state of the polymer segments, which was caused by strong electrostatic interactions from the charged groups in the repeat units. Adjusting the UCST value to a usable range is the direction in which scientists have been working. Although increasing molecular weight (M_n) is effective, more stringent requirements for synthesis conditions and the lack of multi-responsiveness are the major reasons limiting polyzwitterion applications. Hence, exploring effective methods to increase the UCST, especially the multi-responsiveness of polyzwitterions, is a top priority.[10] Roth et al. reported a comparative study of the aqueous solution behavior of sulfobetaine homopolymers and copolymers on how to offer a much larger temperature and salt concentration range for sharp, reproducible UCST transitions.[11] Chen et al. reported that copolymerization of DMAPS with 2-(diisopropylamino)ethyl methacrylate (DPA) imparts dual-responsiveness to polyzwitterions,[12] whose UCST increased from 36 °C at neutral pH to 48 °C at pH 3. Therefore, there is much interest in exploring effective design and synthesis of the polyzwitterions with a wide, adjustable range of UCST and fast responsiveness.

Recently, through reversible-deactivation radical polymerizations (RDRPs), researchers could manipulate the topological structure of polymers to optimize the critical aggregation state.[13-21] Among them, the more compact conformation and three-dimensional spheroidal shape of the star polymer give it special physical-chemical properties,[22,23] such as smaller hydrodynamic volume and diffusion coefficient, lower viscosity, low glass transition temperature, and high functionality.[24-26] Whittaker et al. synthesized *N*-isopropylacrylamide (NIPAM) star polymers through the use of an 4-arm RAFT agent. The lower critical solution temperature (LCST) transitions of these star-shaped PNIPAM were significantly depressed by the presence of the hydrophobic star core.[27] Zhang et al. synthesized the star-shaped thermo-responsive block copolymers of hydrophilic cationic monomer 2-(dimethylamino) ethyl methacrylate (DMAEMA) and DMAPS by modified cyclodextrin initiator.[28] A tunable critical aggregation temperature with varying arm densities or pH values was obtained in NaCl solutions. Biocompatibility evaluations showed the star polymers could effectively reduce

[a] *Beijing Advanced Innovation Center for Soft Matter Science and Engineering, College of Materials Science and Engineering, Beijing University of Chemical Technology, Beijing 100029, China.*
[b] *Institute for Materials Discovery and Department of Chemistry, University College London, WC1H 0AJ London, UK.*
[c] *State Key Laboratory of Organic-Inorganic Composites, Beijing University of Chemical Technology, Beijing 100029, China.*
[d] *School of Chemistry, Monash University, Clayton, Victoria 3800, Australia*
Electronic Supplementary Information (ESI) available: [details of any supplementary information available should be included here]. See DOI: 10.1039/x0xx00000x

the adsorption of bovine serum albumin (BSA) in phosphate buffer saline (PBS) solution and showed insignificant cytotoxicity to MCF-7 cells. However, more research has been based on the assembly of topological structures, neglecting the manipulation of thermo-responsiveness of star-shaped polymers, even rare works focused on the UCST star-shaped polymers.[29] To the best of our knowledge, there are still significant areas of improvement: (i) it is still difficult to attain a practical phase transition temperature suitable for ambient temperature applications after changing the topological structure of homopolymers; (ii) lack of reproducibility due to complicated design and synthetic steps of multi-component polymers; (iii) large hydrodynamic volume due to multiple components or large hydrophobic cores makes the material unsuitable for applications such as coatings, adhesives and drug release; and (iv) fast responsiveness and wide adjustable range are typically incompatible.

Herein, star-shaped PDMAPS with functional end-group were synthesized by RAFT polymerization. In this work, a star-shaped polymer with adjustable UCST and fast responsiveness was prepared by an "arm-first" approach involving RAFT polymerization of PDMAPS as a macroRAFT agent. Comparing to linearly-shaped PDMAPS, the UCST of star-shaped PDMAPS (star-PDMAPS) was greatly increased and could be manipulated by controlling the feed ratio of the macroRAFT agent to crosslinker MBA. Furthermore, sensitive pH-responsiveness of star-shaped PDMPAS was achieved along with a more significant adjustable UCST range (over 36 °C from pH 3 to pH 10) due to the multiple carboxylic acid end-groups. We first provided a simple and effective method for synthesizing a novel material with low hydrodynamic volume, fast responsiveness, high UCST, and wide adjustable UCST range. These star polymers are expected to be used in surface modification, drug delivery and nanoreactor applications thanks to the dual-responsiveness and good rheological properties.[13]

Results and discussion

Synthesis of star-PDMAPS

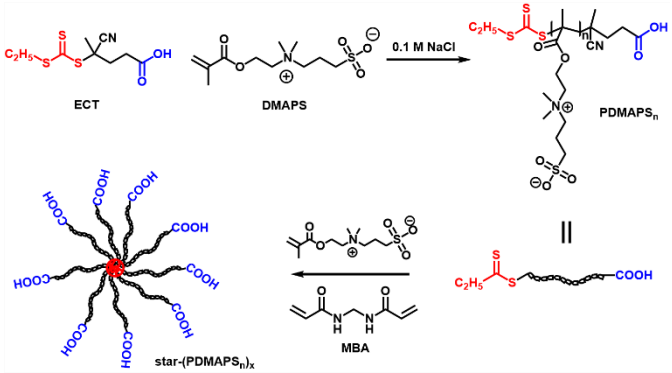

Scheme 1 Synthesis of star-PDMAPS via "arm-first" RAFT polymerization.

$PDMAPS_n$ homopolymers and star-$(PDMAPS_n)_x$ polymers with different number of arms were synthesized by following the synthetic route in Scheme 1, where n represents the degree of polymerization (DP) and x is the rounded number of arms (N_{arm}). Synthetic procedures and summary of characterization data of polymers are shown in the supporting information (Table S1) and Figure 1. ^{1}H NMR spectra of MBA, DMAPS, $PDMAPS_{80}$ and star-$(PDMAPS_{80})_8$ samples are shown in Figure 1. The (meth)acrylic characteristic peaks of the DMAPS and MBA did not appear in the star-$(PDMAPS_{80})_8$ spectra, which indicate a high monomer conversion and reaction degree of the crosslinker. Additionally, Small-angle X-ray Scattering (SAXS) is a useful characterization to show more information about the polymer conformation in aqueous solutions.[30] According to the previous studies,[31,32] SAXS and model fitting were carried out to identify the star-shaped feature of the synthesized polymer (Figure S1). The experimental details were shown in Supporting Information. A GausPoly unimer model was found to fit linearly-shaped $PDMAPS_{80}$ well, while the curve of star-$(PDMAPS_{80})_8$ displays a best-fit for a DozierStar polymer model.

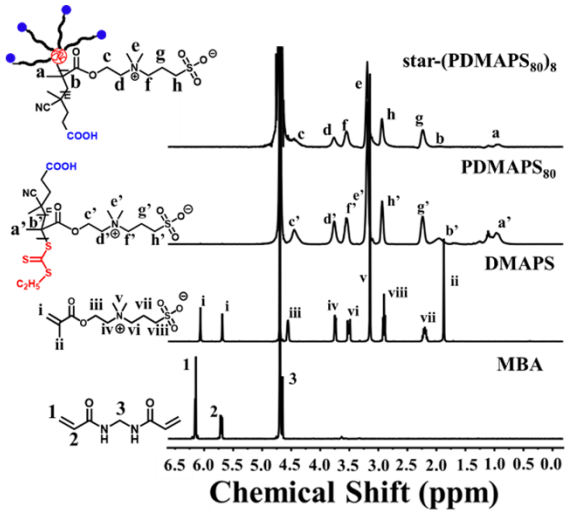

Figure 1 ^{1}H NMR spectra of MBA, DMAPS, $PDMAPS_{80}$ (after purification) and star-$(PDMAPS_{80})_8$ (before purification) in D_2O.

The arm conversion was estimated from unpurified star-$(PDMAPS_{80})_8$ GPC trace in Figure 2. The shoulder peak on the curve can be considered as an untransformed polymer arm, whose retention time is the same as $PDMAPS_{80}$ (at ~18.7 min). After peak division and integral calculation, the arm conversion of all star-shaped polymers is over 90 % (Table S1). Herein the N_{arm} was determined along with the arm conversions and feed ratios of [crosslinker]: [macroRAFT], which are shown in Table S1. To ensure that the average number of arms of the studied star polymer is regular and close to integers, the feed ratio is adjusted slightly to reach the target arm number. The purified star-$(PDMAPS_{80})_8$ polymer was also analyzed by GPC (Figure 2), which showed a high molecular weight and low molar mass distribution (M_n= 67800, $Đ$= 1.13). The obtained M_n of the star polymers from GPC was less than the modelled M_n, according

to N_{arm}, which is due to the small hydrodynamic volume and it was also found by Armes et al. that the molecular weight of polysulfobetaines obtained by the aqueous GPC was comparatively smaller.[33]

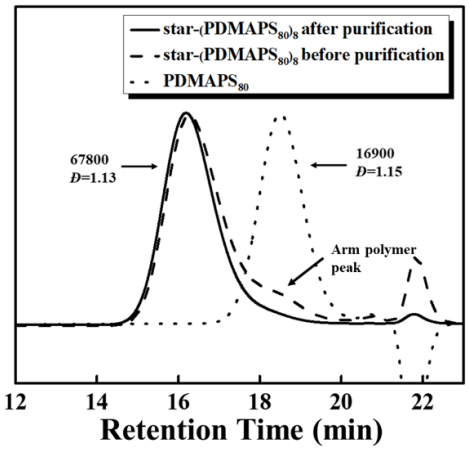

Figure 2 GPC traces of $PDMAPS_{80}$ and star-$(PDMAPS_{80})_8$ before and after purification.

Thermo-responsiveness of star-PDMAPS aqueous solution

Phase-transition behavior and UCST of the purified polyzwitterions were characterized using UV-visible spectrophotometry (Figure 3). According to the spectra, the linearly-shaped polymer $PDMAPS_{80}$ showed an abrupt change in turbidity near 6 °C. After crosslinking, the UCST of the 6-arm and 8-arm star-PDMAPS were significantly increased over the arm polymer $PDMAPS_{80}$ from 6 °C to 16 °C and 23 °C, respectively. This enhancement could be caused by an increase in M_n which leads to enhanced intermolecular electrostatic interactions.

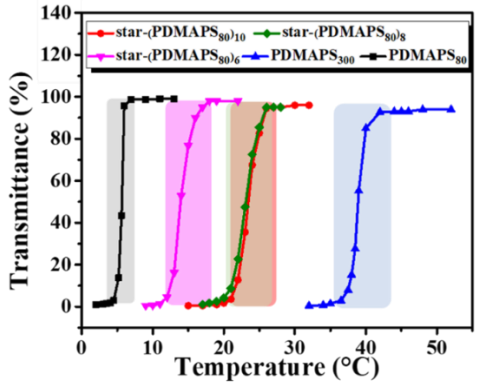

Figure 3 Thermo-responsive properties of $PDMAPS_{80}$, $PDMAPS_{300}$, star-$(PDMAPS_{80})_6$, star-$(PDMAPS_{80})_8$ and star-$(PDMAPS_{80})_{10}$ aqueous solutions (10 mg mL^{-1}) under neutral conditions.

Moreover, the influence of core-shell nanostructure cannot be neglected. To address this, a linearly-shaped $PDMAPS_{300}$ with the similar M_n to star-$(PDMAPS_{80})_8$ was synthesized as a comparison (Figure S2a, Figure 2). The general disadvantage of polyzwitterions is that after the M_n increase, the phase change window became wider, indicating a slower transition (Figure 3) which was also proved by Chang et al.[34] Notably, the conformational advantage of star polymers can overcome the disadvantage of slowing the response speed caused by the increasing M_n. The phase transition windows of star-shaped polymers are still narrow with the molecular weight increases (Figure 3), although the star-$(PDMAPS_{80})_8$ exhibited a lower UCST than linearly-shaped $PDMAPS_{300}$ at similar M_n. It provides an excellent prerequisite for the synthesis of fast responsiveness and wide adjustable range pH-responsive polymer. For star polymers with varied arm numbers, an increase in M_n (Figure S2b, c) can lead to a denser star polymer with more arms. Nevertheless, the UCST did not continuously increase as N_{arm} increased. The UCST of star-$(PDMAPS_{80})_{10}$ is around 24 °C, which is also similar to that of star-$(PDMAPS_{80})_8$ (Figure 3), although the M_n of the star polymer increased with the number of arms.

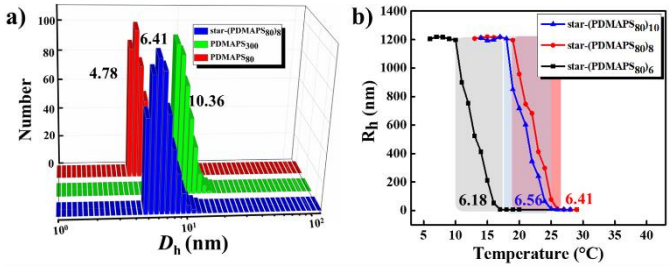

Figure 4 (a) Hydrodynamic diameters (number-average) of $PDMAPS_{80}$, $PDMAPS_{300}$ and star-$(PDMAPS_{80})_8$ aqueous solutions (10 mg mL^{-1}) obtained by DLS measurement at 50 °C. (c) Varied-temperature measurement of hydrodynamic radii (number-average) of star-$(PDMAPS_{80})_6$, star-$(PDMAPS_{80})_8$ and star-$(PDMAPS_{80})_{10}$ aqueous solutions (10 mg mL^{-1}) obtained by DLS.

Herein, DLS measurements were used to characterize the hydrodynamic size (D_h) above the UCST (Figure 4a). The D_h of star-$(PDMAPS_{80})_8$ is bigger than that of $PDMAPS_{80}$ due to the branched conformation. A smaller D_h was observed when compared to $PDMAPS_{300}$, indicating a denser structure. Varied-temperature measurement of D_h was performed to investigate the aggregation behavior of star polymers (Figure 4b). The star polymers with different numbers of arms all showed similar behavior that the aggregate size rapidly decreased with increasing temperature. Notably, the rheological data also indicate that, at a comparatively high solid content (200 mg mL^{-1}), the star polymer solution showed consistently lower viscosity under different shear rates, while the star polymer solution beyond UCST acted as a Newtonian fluid, and the homopolymers exhibited a shear-thinning phenomenon (Figure 5).

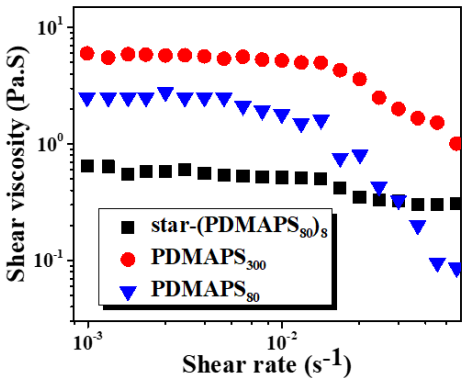

Figure 5 Steady-shear viscosity profiles for $PDMAPS_{80}$, $PDMAPS_{300}$ and star-$(PDMAPS_{80})_8$ aqueous solutions (200 mg mL^{-1}) at 50 °C.

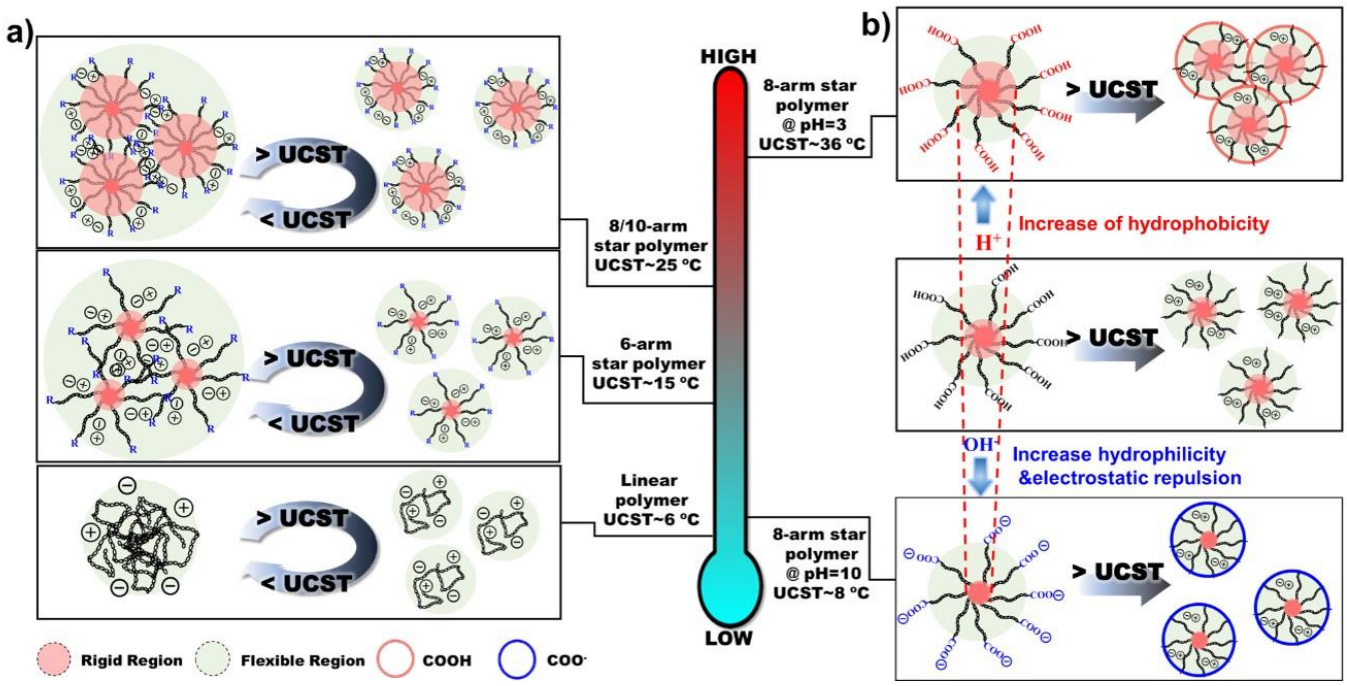

Scheme 2 a) Conformation effects on thermo-responsiveness of PDMAPS. b) Schematic diagram of the response of star-shaped polymers' end-groups with respect to pH.

Based on the above observation, we hypothesize that the star polymer formed by crosslinking was composed of a core with certain rigidity and flexible arm chains (Scheme 2a). The UCST originates from the flexible chains in the flexible region while the chains in the rigid crosslinked region contribute very little to the lack of mobility and difficulty to contact other chains. For star polymers with varied arm numbers, the UCST did not increase continuously as N_{arm} increased. According to our hypothesis, the reason is that the rigid region increased as the number of arms increased, which finally led to the attenuation of effective area for flexible arm chains to interact (Scheme 2a).

pH-responsiveness of star-PDMAPS aqueous solution

As mentioned above, the introduction of other polymer components through copolymerization can bring stimuli-responsiveness, which can enable adjustable UCST. Meanwhile, many studies have shown that polymer end-groups can play a role in regulating polymer properties.[35-38] After realizing the rich end cardinality of star polymers, specifically carboxylic acid end-groups in star-PDMAPS, the pH-responsiveness of PDMAPS and star-PDMAPS were studied in details. Containing several times more carboxyl end-groups per macromolecule than linearly-shaped PDMAPS, temperature responsiveness of star-PDMAPS is expected to be more sensitive to pH value.

First, the pK_a of the terminal carboxylic acid group should be identified. Acid titration studies of the ECT RAFT agent in aqueous solution (Figure S3) indicated that the pK_a is approximately 4.2, which is consistent with that expected for a free carboxylic acid end-group. Then star polymer solutions with different numbers of arms were prepared in aqueous solutions of varying pH values (10 mg mL^{-1}) to test UCST, where the pH was adjusted by HCl or NaOH before preparation. The UCST data of $PDMAPS_{80}$ and three star-shaped polymers at different pH are shown in Figure S4. To investigate the end-group effect of star-shaped polymers on thermo-responsiveness, the UCST data of $PDMAPS_{300}$ and star-$(PDMAPS_{80})_8$ are shown in Figure 6, where a wider range of pH

manipulated UCST values of star-$(PDMAPS_{80})_8$ were observed at a similar M_n. The UCST of star-$(PDMAPS_{80})_8$ could be adjusted from 9 °C to 37 °C by changing the pH due to the protonation/deprotonation of the carboxylic group.

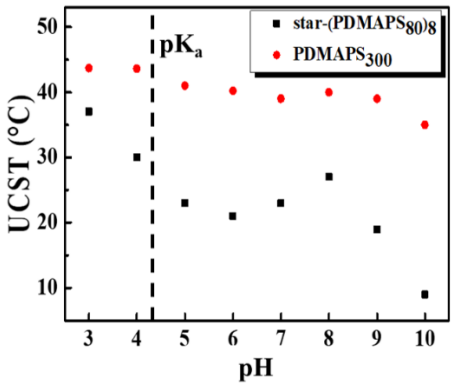

Figure 6 UCST of the $PDMAPS_{300}$ and star-$(PDMAPS_{80})_8$ aqueous solutions (10 mg mL^{-1}) under different pH values.

An increasing trend of UCST was observed in the range of pH 8-9, which has also been shown in the $PDMAPS_{80}$ sample. This was due to the increased electrostatic interactions between the ionized carboxyl end-groups and zwitterionic segments. To confirm this, the effect of Na^+ and Ca^{2+} on thermo-responsive behaviors of $PDMAPS_{145}$ under basic condition was examined (Figure S5). The difference in responsive behavior (pH 7 to pH 10) can be ascribed to the specific interactions between the carboxylic acid group and Ca^{2+}.[35] According to our hypothesis (Scheme 2), another possible reason is that as the end-groups were gradually ionized, the electrostatic repulsion increased leaded to the enlarging chain spacing with a decrease in the rigid region and an increase in the amount of flexible chains (Scheme 2b), finally caused an increase in UCST. In other words, carboxylic end-groups could also affect UCST by changing the chain conformation. However, as the pH continued to increase, the increased hydrophilicity brought by the ionization of the end-groups caused the polymer coils deaggregation and reduce the UCST.

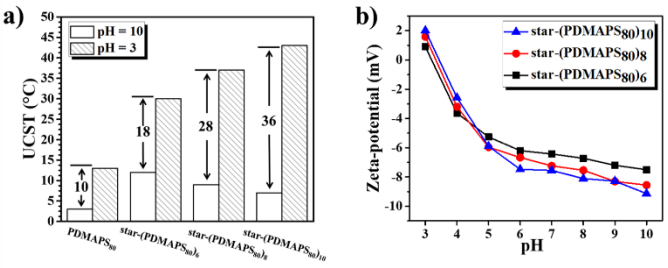

Figure 7 (a) UCST of the $PDMAPS_{80}$, star-$(PDMAPS_{80})_6$, star-$(PDMAPS_{80})_8$ and star-$(PDMAPS_{80})_{10}$ aqueous solutions (10 mg mL^{-1}) at pH 3 and pH 10. (b) Zeta-potential results (50 °C) of the star-$(PDMAPS_{80})_6$, star-$(PDMAPS_{80})_8$ and star-$(PDMAPS_{80})_{10}$ aqueous solutions (10 mg mL^{-1}) with different pH values.

As expected, the response-temperature sensitivity of star-shaped PDMAPS to pH increased with the number of arms (Figure 7a). For example, the UCST adjustable range of star polymers by changing the pH from 3 to 10, was gradually increasing from 18 to 36 degrees with the arm number increase. DLS and zeta-potential measurements were conducted beyond UCST as a function of solution pH for star-$(PDMAPS_{80})_6$, star-$(PDMAPS_{80})_8$ and star-$(PDMAPS_{80})_{10}$ samples (Figures 7b and S4) to further confirm the end-group effect. Under an acidic condition of pH= 3, which is lower than the pK_a of the carboxyl group on ECT, the star-$(PDMAPS_{80})_{10}$ exhibited the highest zeta-potential value (Figure 7b). Under such conditions, the carboxyl end-groups were mainly protonated that result in increased hydrophobicity, leading to the aggregations of polymer segments and increased D_h values (Figure S6). The increase in D_h under acidic pH should be due to aggregation/ clustering rather than an increase in size of individual star polymers. In fact, the size of individual star polymer should be larger under basic pH due to charge repulsion and a thicker hydration shell / electric double layer.[13] Conversely, under basic conditions (pH= 10), larger numbers of carboxyl end-groups introduced by more arms could be ionized. When the number of star arms increased in ionization, a decrease in D_h was observed as a result of electrostatic repulsion and increased hydrophilicity (Scheme 2b).

Conclusions

In conclusion, dual-responsive star polyzwitterions containing abundant peripheral carboxyl end-groups were synthesized by RAFT polymerization using an “arm-first” approach. In contrast to precedent examples in the literature, significant raise of UCST was observed for the star-shaped polymer after crosslinking. Compared to linear PDMAPS at the same M_n, star-shaped PDMAPS exhibited a wide range of pH-adjustable UCST values and excellent rheological properties in aqueous. DLS and zeta-potential measurements were used to support the great influence of end-group effects on the pH and thermo-responsiveness. While the improved responsiveness was decent, more techniques must be developed to achieve more precise UCST control, such as accurate control and quantitative end-group measurements in the future. Eventually, a material that is highly sensitive to pH changes from which UCST can be regulated, must be synthesized. The unique conformation of star-shaped polyzwitterions and their excellent rheological properties allow for use in drug carriers and controlled-release applications.

Experimental

Materials

3-((2-(Methacryloyloxy) ethyl) (dimethyl) ammonio) -1-propanesulfonate (DMAPS, 99%), 4,4’-azobis(4-cyanopentanoic acid) (ACVA, V-501; 99%), *N,N*-dicyclohexylcarbodiimide (DCC, 99%), *N,N*’-methylenebis (acrylamide) (MBA, 99%) were purchased from Sigma-Aldrich

and were used as received. The RAFT agent 4-cyano-4-(ethylthiocarbonothioylthio) pentanoic acid (ECT) was synthesized according to previous report.[39] All other reagents and chemicals were purchased from commercial sources and were used as received without further purification.

Characterizations

^{1}H NMR spectra for structural assignments and polymer conversion were obtained on a Bruker Avance 400 MHz spectrometer. Chemical shifts (δ) are quoted in parts per million (ppm), using a residual deuterated solvent as internal standard (D_2O at 4.79 ppm, $CDCl_3$ at 7.26 ppm). Abbreviations used in the description of resonances are: s (singlet), d (doublet), t (triplet), q (quartet), br (broad). Coupling constants (J) are quoted to nearest 0.1 Hz. The molecular weight was measured by using a Shimadzu GPC system equipped with a SIL-20A autosampler, a refractive index detector, three Shodex KF-805L columns (8 × 300 mm, 10 μm, 5000 Å) and one Shodex KF-801 column (8 × 300 mm, 6 μm, 50 Å) using water (containing 0.1 M sodium chloride) as the eluent at 40 °C with a flow rate of 0.5 mL min^{-1}. The GPC calibration was accomplished with low dispersity dextran standards. Turbidity measurements were performed on a Hitachi U-3900H UV-vis spectrophotometer equipped with a temperature controller in quartz cuvettes at a wavelength of 550 nm with heating/cooling rates of 1 °C min^{-1}. The samples (10 mg mL^{-1}) were gradually heated from a lower temperature and equilibrated at each selected temperature for 1 min prior to transmittance measurement. Transmittance (%) was plotted against temperature, and cloud points (CP) were determined at the median of transmittance change. The average size and zeta-potential of polymers were analyzed by a Brookhaven Nanobrook Omni (DLS) at 50 °C using a monochromatic coherent He–Ne laser (640 nm) as the light source and a detector that detected the scattered light at an angle of 90°. At 50 °C, the polymers were well dissolved in the solution and the electrostatic interaction between polymer segments were weakened to better examine the effect of end-group on polymer segments. All data were averaged over three consecutive runs. Rheological behaviors of samples were measured with a Kinexus Pro rheometer (Malvern Instruments Ltd.) using a parallel plate of 25 mm diameter and plate-to-plate distance of 0.5 mm, covering a frequency rate from 0.1 rad s^{-1} to 100 rad s^{-1} under 50 °C. The concentrations of polymer solutions were 200 g L^{-1}, and the pH is neutral.

Synthesis of linearly-shaped Poly(3-dimethyl(methacryloyloxyethyl) ammonium propane sulfonate) (PDMAPS$_n$) by ECT. $PDMAPS_{80}$ was synthesized by the following several steps as an example. The molar ratio of [M]:[ECT]:[I]= 800/10/1, DMAPS (0.14 g, 0.5 mmol), ACVA (0.00063mmol, prepared by 177 μL of a stock solution of 1 mg mL^{-1}), and ECT (1.64 mg, 0.0063mmol) were dissolved in sodium chloride solution (0.1 M). Then added the solution into the Schlenk tubes after titrating sodium hydroxide solution (0.1 M). The tubes were sealed and the oxygen was removed after three times freeze-evacuate-thaw cycles. Then performed the polymerization at 70 °C for 24 h. The polymers were purified by dialysis (MWCO of 3000) against Milli-Q water and freeze-dried. $PDMAPS_{145}$ and $PDMAPS_{300}$ were also synthesized following this procedure by changing the molar ratio of [M]:[ECT] to 150:1 and 300:1.

Synthesis of star-shaped Poly(3-dimethyl(methacryloyloxyethyl) ammonium propane sulfonate) (star-(PDMAPS$_n$)$_x$) by "arm first" method. RAFT polymerization was performed to synthesize star-$(PDMAPS_{80})_8$ by $PDMAPS_{80}$ as a macroRAFT agent following the similar synthetic steps as the $PDMAPS_n$. The ratio [macroRAFT]:[ACVA]:[DMAPS]:[MBA] was adjusted to 1.0:0.2:6.0:8.5. The N_{arm} was determined along with the arm conversions and feed ratios of [crosslinker]: [macroRAFT]. By taking advantage of the difference between the star-shaped polymers' UCST and the "arm" polymers' UCST, the star-shaped polymers with low poly-dispersities were obtained by centrifugation (10^4 rpm) at 10 °C and freeze-drying of the precipitate. To investigate the influence of arm numbers to thermal-responsiveness, different [crosslinker]:[macroRAFT] ratios (Table S1) were selected to synthesize star-$(PDMAPS_{80})_6$ and star-$(PDMAPS_{80})_{10}$.

Conflicts of interest

There are no conflicts to declare.

Acknowledgements

This work was supported by the National Natural Science Foundation of China (21704001), the Fundamental Research Funds for the Central Universities (buctrc201724) and the Beijing Advanced Innovation Center for Soft Matter Science and Engineering. Z. S. gratefully acknowledges the scholarship from Graduate School of Beijing University of Chemical Technology. We also appreciate the linguistic assistance provided by TopEdit (www.topeditsci.com) during the preparation of this manuscript.

Notes and references

1 E. L. Foster, Z. Xue, C. M. Roach, E. S. Larsen, C. W. Bielawski, K. P. Johnston, *ACS Macro Lett*., 2014, **3**, 867-871.
2 Q. Shao, S. Y. Jiang, *Adv. Mater*., 2015, **27**, 15-26.
3 K. Seetho, S. Zhang, K. A. Pollack, J. Zou, J. E. Raymond, E. Martinez, K. L. Wooley, *ACS Macro Lett*., 2015, **4**, 505-510.
4 Z. Li, H. L. Tang, A. C. Feng, S. H. Thang, *Prog. Chem.,* 2018, **30**, 1097-1111.
5 F. G. Xu, D. D. Wu, Y. J. Huang, H. Wei, Y. Gao, X. L. Feng, D. Y. Yan, Y. Y. Mai, *ACS Macro Lett*., 2017, **6**, 426-430.
6 H. C. Hung, P. Jain, P. Zhang, F. Sun, A. Sinclair, T. Bai, B. Li, K. Wu, C. Tsao, E. J. Liu, H. S. Sundaram, X. Lin, P. Farahani, T. Fujihara, S. Y. Jiang, *Adv. Mater*., 2017, **29**, 1700617.
7 Z. Y. Lei, P. Y. Wu, *Nat. Commun*., 2019, **10**, 3429.
8 D. Roy, W. L. Brooks, B. S. Sumerlin, *Chem. Soc. Rev*., 2013, **42**, 7214-7243.
9 V. Hildebrand, A. Laschewsky, E. Wischerhoff, *Polym. Chem*., 2016, **7**, 731-740.
10 J. Niskanen, H. Tenhu, *Polym. Chem*., 2017, **8**, 220-232.
11 Y. C. Zhu, J. M. Noy, A. B. Lowe, P. J. Rot, *Polym. Chem*., 2015, **6**, 5705-5718.

12 C. Y. Chen, H. L. Wang, *Macromol. Rapid Comm.*, 2014, **35**, 1534-1540.
13 J. M. Ren, T. G. McKenzie, Q. Fu, E. H. H. Wong, J. T. Xu, Z. S. An, S. Shanmugam, T. P. Davis, C. Boyer, G. G. Qiao, *Chem. Rev*., 2016, **116**, 6743-6836.
14 T. X. Shen, J. J. Wang, H. Zou, W. Z. Yuan, *Polym. Chem.*, 2014, **5**, 3968-3971.
15 H. Zou, W. Z. Yuan, *Polym. Chem*., 2015,**6**,2457-2465.
16 M. Huo, Z. Y. Wan, M. Zeng, Y. Wei, J. Y. Yuan, *Polym. Chem.*, 2018, **9**, 3944-3951.
17 M. Huo, M. Zeng, D. C. Wu, Y. Wei, J. Y. Yuan, *Polym. Chem.,*2018, **9**, 912-919.
18 A. M. Jazani, N. Arezi, C. Shetty, S. H. Hong, H. W. Li, X. T. Wang, J. K. Oh, *Polym. Chem.*, 2019, **10**, 2840-2853.
19 K. K. Bawa, A. M. Jazani, C. Shetty, J. K. Oh, *Macromol. Rapid Comm*., 2018, **39**, 1800477.
20 M. Wang, B. Choi, Z. H. Sun, X. H. Wei, A. C. Feng, *Chem. Comm*., 2019, **55**, 1462-1465.
21 M. Wang, B. Choi, X. H. Wei, A. C. Feng, *Polym. Chem*., 2018, **9**, 5086-5094.
22 Y. Shi, X. S. Cao, D. Q. Hu, H. F. Gao, *Angew. Chem. Int. Edit*., 2018, **57**, 516-520.
23 Y. Sh., R. W. Graff, X. S. Cao, X. F. Wang, H.F. Gao, *Angew. Chem. Int. Edit*.,2015, **127**, 7741-7745.
24 X. P. Miao, Y. S. Guo, L. F. He, Y. Meng, X. Y. Li, *Chinese J. Polym. Sci*, 2015, **33**, 1574-1585.
25 C. Chen, F. X. Kong, X. H. Wei, S. H. Thang, *Chem. Commun.,* 2017, **53**, 10776-10779.
26 N. Xue, X. P. Qiu, Y. G. Chen, T. Satoh, T. Kakuchi, F. M. Winnik, *J. Polym. Sci. Pol. Phys*., 2016, **54**, 2059-2068.
27 R. Plummer, D. J. T. Hill, K. A. Whittaker, *Macromolecules*., 2006, **39**, 8379-8388.
28 M. M. Zhang, W. Shen, Q. Q. Xiong, H. W. Wang, Z. M. Zhou, W. J. Chen, Q. Q. Zhang, *RSC Adv*., 2015, **5**, 28133-28140.
29 C. Zhao, Z. Ma, X. X. Zhu, *Prog. Polym. Sci.*, 2019, **90**, 269-291.
30 J. P. Li, A. Q. Jiao, S. Chen, Z. Z. Wu, E. B. Xu, Z. Y. Jin, *J. Mol. Struct*., 2018, **1165**, 391-400.
31 S. Bekhradnia, J. S. Diget, T. Zinn, K. Zhu, S. A. Sande, B. Nyström, R. Lund, *Macromolecules*, 2015, **48**, 2637-2646.
32 J. Lyngsø, N. Al-Manasir, M. A. Behrens, K. Zhu, A. L. Kjøniksen, B. Nyström, J. S. Pedersen, *Macromolecules*, 2015, **48**, 2235−2243.
33 K. E. B. Doncom, N. J. Warren, S. P. Armes, *Polym. Chem*., 2015, **6**, 7264-7273.
34 Y. J. Shih, Y. Chang, *Langmuir*, 2010, **26**, 17286-17294.
35 C. Chen, X. F. Guo, J. H. Du, B. Choi, H. L. Tang, A. C. Feng, S. H. Thang, *Polym. Chem*., 2019, **10**, 228-234.
36 H. Ren, D. Chen, Y. Shi, H. Yu. Fu. F, F. Z, W. T. Yang, *Macromolecules*, 2018, **51**, 3290-3298.
37 J. R. Lovett, N. J. Warren, L. P. D. Ratcliffe, M. K. Kocik, S. P. Armes, *Angew. Chem. Int. Edit*., 2015, **54**,1279-1283.
38 S. Y. Khor, N. P. Truong, J. F. Quinn, M. R. Whittaker, T. P. Davis, *ACS Macro Lett.,* 2017, **6**, 1013-1019.
39 X. Y. Pan, F. M. Zhang, B. Choi, Y. Luo, X. F. Guo, A. C. Feng, S. H. Thang, *Eur. Polym. J*., 2019, **115**, 166-172.